Brownian motion-induced amplitude noise in vapor-cell frequency standards

New Journal of Physics
The open access journal at the forefront of physics

Deutsche Physikalische Gesellschaft DPG IOP Institute of Physics

PAPER • OPEN ACCESS

Brownian motion-induced amplitude noise in vapor-cell frequency standards

To cite this article: S Micalizio *et al* 2020 *New J. Phys.* **22** 083050

New Journal of Physics
The open access journal at the forefront of physics

Deutsche Physikalische Gesellschaft DPG
IOP Institute of Physics

Published in partnership with: Deutsche Physikalische Gesellschaft and the Institute of Physics

OPEN ACCESS

RECEIVED
4 May 2020

REVISED
29 June 2020

ACCEPTED FOR PUBLICATION
9 July 2020

PUBLISHED
18 August 2020

PAPER

Brownian motion-induced amplitude noise in vapor-cell frequency standards

S Micalizio[1], **A Godone, M Gozzelino and F Levi**

INRIM, Istituto Nazionale di Ricerca Metrologica, Strada delle Cacce 91, 10135, Torino, Italy
[1] Author to whom any correspondence should be addressed.

E-mail: s.micalizio@inrim.it

Keywords: Brownian motion, vapor cell frequency standard, frequency stability, laser relative intensity noise

Abstract

We demonstrate that the Brownian motion of alkali metal atoms in buffer gas gives rise to a significant source of frequency instability in vapor cell clocks. We consider, in particular, laser pumped cell devices working in pulsed operation and using a resonant Gaussian light beam to detect the clock transition. It is well known that the diffusion motion through the buffer gas results from many random walks performed by the atoms, as a consequence of the collisions with other atoms/molecules. Owing to this random-walk behavior, the atoms explore different intensity regions of the Gaussian laser beam, reducing the forward light transmission and causing amplitude fluctuations at the photodetector. The contribution of this so called transit noise to the clock frequency stability turns out in the low 10^{-14} region for a centimeter-scale cell, at the same level of other amplitude noises, like laser relative intensity noise and shot noise. As a consequence, even if it is not the main source of instability in currently used vapor cell clocks, Brownian motion-induced noise represents a novel source of frequency fluctuations and it should be accounted for in the clock stability budget. A preliminary evaluation of the transit noise is also reported for microcell devices.

1. Introduction

Laser pumped vapor cell frequency standards have recently reached outstanding performances in terms of frequency stability [1]. These results have been obtained with either hot [2–5] or cold atoms [6, 7], and in most cases, operating the clocks in pulsed regime [8–11]. Pulsing the different clock operation phases has been recognized as an effective technique to significantly reduce the transfer of laser instabilities to the atom clock transition, with a consequent improvement of the long term stability.

In hot atom-based devices, it is of primary importance to add an inert buffer gas to the alkali atom cell. In fact, gases such as Ar, N_2 and Ne prevent the relaxation of polarized alkali-metal atoms on the cell walls and at the same time localize the atoms suppressing the Doppler broadening at microwave wavelengths. In centimeter-scale cells, buffer gas pressures in the range 10–30 Torr are commonly used so that the mean free path of the alkali atoms turns out to be of the order of 1–10 μm and the atoms make a random walk diffusive motion through the buffer gas.

It is well known that the buffer gas causes relaxation of the atomic coherence and shifts the clock transition frequency [12]. In addition, this shift is temperature sensitive and can be an important source of frequency instability, mainly in the medium-long term period. A tight control of the cell temperature is then required.

In this paper we show that the short-term stability as well is not immune to the buffer gas action. Specifically, during their random-walk motion across the laser beam, the atoms absorb photons from the detection laser causing fluctuations in the amplitude of the transmitted light, a phenomenon known as transit noise [13]. The associated spectrum can be theoretically deduced under the hypothesis of atomic Brownian motion and results in good agreement with the experiments done with Rb atoms in N_2 as buffer gas.

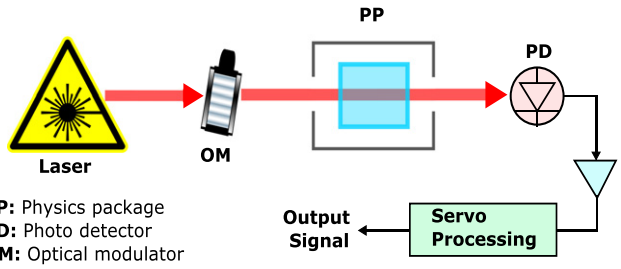

Figure 1. Schematic clock setup considered in the paper.

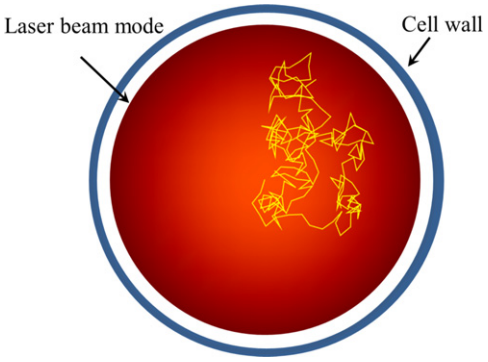

Figure 2. Cross-section view of a cylindrical cell of radius R showing an atom making random walk (yellow trace) and probing different intensity regions of a Gaussian laser beam. Brighter beam colors correspond to higher intensities.

Here we extend the analysis to vapor-cell frequency standards and we prove for the first time that this buffer gas-induced random walk performed by the atoms can represent a considerable noise source, comparable or even larger than the shot noise, so far usually identified as the ultimate noise limit.

The paper is organized as follows. In section 2 we introduce the phenomenon of transit noise and we derive an expression of its spectrum for an optically thick atomic vapor. In section 3 the impact of the transit noise on the frequency stability is evaluated for high performing vapor cell clocks that adopt cells with the size of the order of centimeters. Section 4 is devoted to microcells and conclusions are reported in section 5.

2. Transit noise spectrum

We consider the vapor-cell arrangement shown in figure 1 that applies to a large variety of cell clocks, including either the pulsed optical pumping (POP) or the pulsed coherent population trapping (PCPT) techniques.

The cell contains the resonant atoms and buffer gas atoms/molecules. The main parameters characterizing the clock cell are its size, the atomic density n at the operation temperature, the buffer gas pressure P_{bg} and the diffusion coefficient D through the buffer gas. Depending on the adopted scheme, the atoms can be submitted to a bichromatic laser field, as in CPT, or to a combination of laser and microwave pulses, as in the POP. In this latter case, the laser is supposed to be monochromatic, an hypothesis well satisfied for narrow line DFB and DBR lasers usually employed in high performing cell clock. What is important for the present discussion is that the detection of the clock transition is done in the optical domain by means of a laser pulse. The laser is supposed to be collimated in the fundamental Gaussian mode (TEM_{00}) with a waist w (which represents the distance from the axis at which the intensity is reduced by a factor e^2) and propagates along the z quantization axis of the physics package.

The atomic motion across the inhomogeneous laser beam gives rise to intensity fluctuations of the transmitted signal used to detect the clock transition (see figure 2). The two-sided (indicated with the apex (2)) power spectral density of this transit noise (tr) has been calculated in [13] for a two-level system:

$$S^{\mathrm{tr},(2)}(\omega) = \frac{\pi n \sigma^2 L I_0^2 w^4}{8D} \mathrm{Re}\left\{-\mathrm{e}^{\mathrm{i}\omega'} \mathrm{Ei}(-\mathrm{i}\omega')\right\} \tag{1}$$

where $\omega' = \frac{w^2}{4D}\omega$, Ei is the exponential-integral function [14], $\omega = 2\pi f$ is the (angular) Fourier frequency, L is the cell length, $I_0 = \frac{2P_L}{\pi w^2}$ is the laser intensity for a Gaussian beam of power P_L, and σ is the photon absorption cross section. We remind that σ depends on the dipole moment d_e and on the (angular) frequency ω_0 of the optical transition through the relation:

$$\sigma = \frac{2d_e^2\omega_0}{\hbar c\epsilon_0\Gamma^*} \tag{2}$$

where $\hbar$, c and ϵ_0 are the (reduced) Planck constant, the speed of light in vacuum and the permittivity of free space, respectively. We observe that equation (2) neglects saturation effects, a condition satisfied in our case since the atoms lifetime in the excited state is very short, of the order of a few ns, due to collisions with buffer gas atoms/molecules.

The excited state relaxation rate Γ^* includes the homogeneous broadening due to buffer gas collisions and the Doppler broadening [15].

Relation (1) has been obtained under the following hypothesis: (1) the optical transition is not saturated; (2) the atomic medium is assumed optically thin, or equivalently the laser intensity is so high to shine uniformly all the cell along z; (3) the laser frequency ω_L is in resonance with the optical transition ($\omega_L = \omega_0$).

When $\omega' \gg 1$, that is when the Fourier frequency f is much larger than the characteristic frequency $f_{tr} \equiv \frac{2D}{\pi w^2}$, (1) can be written as

$$S^{tr,(2)}(f) = \frac{2n\sigma^2 LP_L^2 D}{\pi^3 w^4}\frac{1}{f^2} \tag{3}$$

by keeping only the leading term in the asymptotic expansion of Ei [14]. Equation (3) defines a random walk process ($\frac{1}{f^2}$) and makes evident the dependence of the spectrum versus the main parameters. This dependence has been found in good agreement with the experimental results [13]; in particular, the spectrum turns out highly sensitive to the beam waist w.

In the limit $|\omega| \to 0$, the spectrum behaves as $S^{tr,(2)}(\omega) \propto -\log|\omega|$ (logarithmic divergence), even if the variance of the statistical process is finite [16].

In order to extend the results reported in [13] to vapor cell frequency standards, some points need to be considered. First, in a clock stability budget, the transit noise is to be compared to other noise sources, like the laser intensity noise, that in general are the outcomes of experiments and expressed in the form of one-sided (indicated with the apex (1)) spectral density. We remind that the relationship between one sided and two-sided spectral densities is $S^{(1)}(f) = 2S^{(2)}(f)$ [17]. Second, differently from [13], the atomic medium is in general thick since we are interested to have a large number of interacting atoms to observe the clock transition with a high signal-to-noise ratio. This is correctly taken into account with the replacement $LI_0^2 \to \int_0^L I^2(z)\mathrm{d}z$ in (1), where $I(z)$ is the intensity profile as the light propagates in the medium along the z axis. Definitely, the general expression of the relative transit noise spectrum can be written as (in the following we will consider one-sided spectra only and the apex (1) will be dropped):

$$S_{AM}^{tr}(\omega) \equiv \frac{1}{P_L^2}S^{tr}(\omega) = \frac{n\sigma^2\int_0^L I^2(z)\mathrm{d}z}{\pi D I_0^2}\Re\left\{-e^{i\omega'}\mathrm{Ei}(-i\omega')\right\}. \tag{4}$$

Extending the theory reported in [13] to an optically thick case as done in equation (4) implicitly assumes that the radial diffusion time is shorter than the longitudinal diffusion time. In order to verify that vapor cell clocks usually satisfy that condition, we observe that an effective radial diffusion time can be defined as:

$$T_R = \frac{w^2}{D}. \tag{5}$$

Similarly, we can introduce an effective longitudinal diffusion time. By assuming for simplicity the Beer–Lambert exponential attenuation law, a longitudinal diffusion time can be defined as:

$$T_L = \frac{16}{[(n\sigma)^2 D]} \tag{6}$$

being $\frac{4}{n\sigma}$ the distance along the beam path where the input laser intensity drops by e^2. Therefore, equation (4) is valid provided $w < 4/(n\sigma)$, a condition satisfied in the clocks discussed in this paper.

3. Transit noise in centimeter size cells

We start considering the setups working with centimeter size cells case where the approximation $f \gg \frac{2D}{\pi w^2}$ holds (see later) and previous equation reduces to:

$$S_{\mathrm{AM}}^{\mathrm{tr}}(f) = \frac{4n\sigma^2 D\int_0^L I^2(z)\mathrm{d}z}{\pi^3 w^4 I_0^2}\frac{1}{f^2}. \tag{7}$$

Two issues should be addressed to determine at which level the transit noise spectrum expressed by (4) or (7) affects the stability of vapor cell clocks.

The first problem concerns the evaluation of the integral in (4) and (7). To do that, we consider the absorption law of a laser signal propagating in a dense atomic medium [18]:

$$\log\frac{\Gamma_{\mathrm{p}}(z)}{\Gamma_{\mathrm{p}}(0)} + \frac{1}{\gamma_1}\left[\Gamma_{\mathrm{p}}(z) - \Gamma_{\mathrm{p}}(0)\right] = -\frac{\alpha z}{\Gamma^*} \tag{8}$$

where $\Gamma_{\mathrm{p}}(0)$ ($\Gamma_{\mathrm{p}}(z)$) is the laser pumping rate at the entrance (at point z) of the cell, γ_1 is the population (longitudinal) relaxation rate and α is the absorption coefficient. Specifically, in (8) and in what follows Γ_{p} is intended to be the optical pumping rate of the laser during the clock transition detection phase. We remind that the optical pumping rate can be expressed in terms of the laser intensity as:

$$\Gamma_{\mathrm{p}}(z) = \frac{Z_0}{\Gamma^*}\left(\frac{d_{\mathrm{e}}}{\hbar}\right)^2 I(z) \tag{9}$$

where Z_0 is the impedance of free space.

In order to provide a practical expression for the transit noise spectrum induced by the atom Brownian motion, we analyze (8) under two asymptotic situations (low and high laser pumping rates, respectively):

$$\begin{aligned} &\Gamma_{\mathrm{p}}(z) = \Gamma_{\mathrm{p}}(0)e^{-\frac{\alpha}{\Gamma^*}z} && \text{for } \Gamma_{\mathrm{p}}(0) \ll \zeta\gamma_1 \\ &\Gamma_{\mathrm{p}}(z) = \Gamma_{\mathrm{p}}(0)\left[1 - \frac{\alpha}{\Gamma^*}\frac{\gamma_1}{\Gamma_{\mathrm{p}}(0)}z\right] && \text{for } \Gamma_p(0) \gg \zeta\gamma_1 \end{aligned} \tag{10}$$

being $\zeta = \frac{\alpha L}{\Gamma^*} = \frac{1}{2}n\sigma L$ the optical thickness of the atomic medium. The first equation in (10) is the well known Beer–Lambert law. Similar equations hold also for CPT, with the difference that the coherence relaxation rate γ_2 replaces γ_1. Taking into account (9) and (10), (7) can be easily integrated, giving:

$$\begin{aligned} &S_{\mathrm{AM}}^{\mathrm{tr}}(f) = \frac{4\sigma D}{\pi^3 w^4}(1 - e^{-2\zeta})\frac{1}{f^2}\ \mathrm{Hz}^{-1} && \text{for } \Gamma_{\mathrm{p}}(0) \ll \zeta\gamma_1 \\ &S_{\mathrm{AM}}^{\mathrm{tr}}(f) = \frac{4n\sigma^2 LD}{\pi^3 w^4}\frac{1}{f^2}\ \mathrm{Hz}^{-1} && \text{for } \Gamma_{\mathrm{p}}(0) \gg \zeta\gamma_1. \end{aligned} \tag{11}$$

Once the laser waist and the cell parameters are fixed, the transit noise spectrum is then expected to lie in a band defined by previous equations; the pumping rate adopted during the detection phase sets the value of the spectrum inside the band.

To provide a numerical evaluation of (11), we consider a cell used for the ^{87}Rb POP clock, as described in [19]. The cell is 2 cm long and contains a mixture of buffer gases, Ar and N_2, at the total pressure of 25 Torr and in the pressure ratio 1.6. According to the data reported in literature [12], the diffusion coefficient D can be estimated as $7.6 \times 10^{-4}\ \mathrm{m^2\ s^{-1}}$. The optical transition of interest is the D_2 line [20, 21] and according to (2) we have $\sigma = 3 \times 10^{-15}\ \mathrm{m^2}$. The cell works at a temperature corresponding to an atomic density of $n = 1 \times 10^{17}\ \mathrm{m^{-3}}$. Assuming a detection performed with a laser beam waist $w = 6$ mm, (11) yield:

$$\begin{aligned} &S_{\mathrm{AM}}^{\mathrm{tr}}(f) = \frac{0.2 \times 10^{-9}}{f^2}\ \mathrm{Hz}^{-1} && \text{for } \Gamma_{\mathrm{p}}(0) \ll \zeta\gamma_1 \\ &S_{\mathrm{AM}}^{\mathrm{tr}}(f) = \frac{1.4 \times 10^{-9}}{f^2}\ \mathrm{Hz}^{-1} && \text{for } \Gamma_{\mathrm{p}}(0) \gg \zeta\gamma_1. \end{aligned} \tag{12}$$

Figure 3 shows the transit noise band defined by the two spectra corresponding to low and high laser pumping rates; the continuous lines in the transit noise spectra show the random walk behavior of (12). The dashed curves, for $f \lesssim \frac{2D}{\pi w^2}$ are directly obtained from (4). We also report typical relative intensity noise (RIN) spectrum of a DFB laser used in the POP clock; according to the experiments [19], for the RIN we measured the following spectrum:

$$S_{\mathrm{AM}}^{\mathrm{RIN}}(f) = \frac{8 \times 10^{-12}}{f} + 3 \times 10^{-15}. \tag{13}$$

The laser RIN is responsible of an additive intensity noise at the clock detector [22]. Depending on the adopted laser source, it may affect the clock short-term stability [23] and its contribution is normally

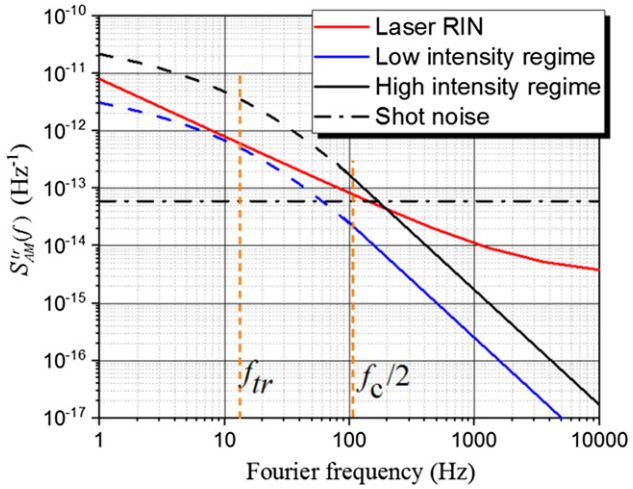

Figure 3. Comparison between transit noise, laser RIN and shot-noise spectra for the POP clock considered in the text. The transit noise is computed for two limiting cases: high and low detection pulse intensities. The figure also shows the two critical frequencies: $f_{\rm tr} = 13.4$ Hz and half the cycle frequency $f_{\rm c}/2 = 107$ Hz, being $T_{\rm c} = 4.65$ ms the cycle time.

evaluated in any laser operated vapor cell clock. Therefore, a comparison with the laser RIN spectrum provides a first information about the importance of the transit noise. It is interesting to note that the cycle frequencies usually adopted in high-performing vapor cell clocks stand in the region 100–300 Hz, exactly where the RIN is comparable to the transit noise spectrum evaluated for the high laser intensity regime. We point out, however, that even more performing lasers with a lower RIN could be used, in that case the transit noise could be comparable to the laser RIN also when the detection occurs in the low pumping regime.

For the same experimental implementation, we can evaluate the shot noise considering that its power spectral density represents a white noise process and can be written as:

$$S^{\rm shot}_{\rm AM}(f) = \frac{2\hbar\omega_{\rm L}}{\eta P_{\rm det}} \tag{14}$$

where η is the quantum efficiency of the detector and $P_{\rm det}$ is the laser power reaching the detector. For the specific example we are considering, the laser power at the exit of the cell and reaching the detector turns out $P_{\rm det} \approx 15\,\mu$W [19]. Assuming $\eta = 0.56$ we have:

$$S^{\rm shot}_{\rm AM}(f) = 6 \times 10^{-14}. \tag{15}$$

Regardless of the specific technique adopted to operate the clock, this comparison then suggests that the transit noise may play a role to determine the clock frequency stability.

The second issue to be addressed is how this noise is transferred to the clock signal, taking into account that the clock works in pulsed regime. In [24] we developed a general approach to evaluate how intensity fluctuations affecting the atomic signal and reaching the photodetector impact on the stability of a pulsed operating clock. We have found that for a given intensity spectrum $S_{\rm AM}(f)$, the contribution to the clock stability (expressed in terms of Allan deviation $\sigma_y(\tau)$) can be written as:

$$\sigma_y(\tau) = \frac{2}{D_{\rm e}}\sqrt{\sum_{k\ \rm odd} \mathrm{sinc}^2\left(\pi\frac{k}{2T_{\rm c}}\tau_{\rm d}\right) S_{\rm AM}\left(\frac{k}{2T_{\rm c}}\right)\frac{1}{\tau}}. \tag{16}$$

In (16), τ is the averaging time, $\tau_{\rm d}$ and $T_{\rm c}$ the detection and the cycle times, respectively; $D_{\rm e}$ is the discriminant of the clock resonance defined as:

$$D_{\rm e} = \pi\frac{C}{1 - C/2}Q_{\rm a} \tag{17}$$

being C the signal contrast and $Q_{\rm a}$ the atomic quality factor.

In (16), $S_{\rm AM}(f)$ can be interpreted as to include all the contributions that add up linearly and that are detected in the form of amplitude fluctuations at the photodetector: the shot noise,the laser RIN, and the transit noise as well.

It is well established that as the laser light propagates through a resonant vapor, laser phase noise (PM) is converted into laser intensity noise (AM). Even if this laser PM–AM conversion [25] may in principle

contribute to the fluctuations of the clock signal, we did not included in the $S_{\rm AM}(f)$. Due to its intrinsic non-linearity, PM–AM conversion deserves a dedicated analysis and will be considered in a following work.

We remind the simplified expressions of (16) when $S_{\rm AM}(f)$ is either white or flicker noise [24]. Assuming the commonly adopted notation where the spectrum is given by the sum of power-law processes $\sum_\alpha h_\alpha f^\alpha$ [12], with h_α appropriate coefficients and α integers ranging from -2 to $+2$, we have:

$$\sigma_y(\tau) = \frac{\sqrt{2h_0}}{\pi\frac{C}{1-C/2}Q_{\rm a}}\sqrt{\frac{T_{\rm c}}{\tau_{\rm d}}}\tau^{-1/2} \tag{18}$$

for white frequency noise and

$$\sigma_y(\tau) = \frac{\sqrt{2}\sqrt{2h_{-1}}}{\pi\frac{C}{1-C/2}Q_{\rm a}}\sqrt{T_{\rm c}}\sqrt{\gamma + \log\left(1.56\,\frac{T_{\rm c}}{\tau_{\rm d}}\right)}\tau^{-1/2} \tag{19}$$

for flicker noise, being γ the Euler–Mascheroni constant.

We can find a more compact expression of (16) also for random walk that is exactly the behavior observed for transit noise, being of the type $\frac{h_{-2}}{f^2}$. Replacing then this law in (16) and taking into account that in pulsed vapor cell clocks $T_{\rm c}/\tau_{\rm d} \gg 1$ is usually satisfied, we obtain:

$$\sigma_y(\tau) \approx \frac{\sqrt{2h_{-2}}}{\frac{C}{1-C/2}Q_{\rm a}}T_{\rm c}\tau^{-1/2}. \tag{20}$$

We point out that despite the transit noise process is random-walk, it affects the clock's stability as white noise. This is due to the detection process which results in a 'whitening' of the noise affecting the clock signal. As an example, we can then provide an evaluation of (20) for a typical implementation of the POP Rb clock. We consider again the cell parameters previously reported; moreover, referring to the measured data reported in [19] we have $C = 0.28$, $Q_{\rm a} = 4.5 \times 10^7$, $\gamma_1 = 360\,{\rm s}^{-1}$, $\tau_{\rm d} = 150\,\mu{\rm s}$ and $T_{\rm c} = 4.65$ ms. In the nominal operating conditions, the laser power adopted during the detection phase corresponds to a pumping rate $\Gamma_{\rm p}(0) = 5.6 \times 10^4\,{\rm s}^{-1}$, whereas the optical thickness of the atomic medium turns out $\zeta \approx 17$. The high power regime holds and (12) and (20) yield:

$$\sigma_y^{\rm tr}(\tau) = 1.8 \times 10^{-14}\tau^{-1/2}. \tag{21}$$

The shot noise contribution to the clock stability can be evaluated by means of (15) and (18) and turns out:

$$\sigma_y^{\rm shot}(\tau) = 4.3 \times 10^{-14}\tau^{-1/2}. \tag{22}$$

Similarly, we can compute the laser RIN contribution taking into account (13) and (19), obtaining:

$$\sigma_y^{\rm RIN}(\tau) = 1.9 \times 10^{-14}\tau^{-1/2}. \tag{23}$$

It is significant to observe that all the three contributions lie in the low 10^{-14} region. Even if the transit noise is one order of magnitude below the current clock performance, it should be evaluated in the stability budget, in the same manner as shot and RIN noises are assessed. Different experimental implementations can easily interchange the role of the considered noise terms.

The evaluation of the transit noise has been done using the data related to a POP Rb clock. The effect of atomic diffusion motion has been also reported for CPT resonances observed either in steady-state or in pulsed regimes [26, 27]. In addition, we note that most performing CPT clocks based either on push–pull [28] or autobalanced-Ramsey techniques reached similar values of contrast and quality factor of the clock resonance. Also, the timing sequence is comparable to that of the POP clock, being mainly limited by the cell properties. Therefore, we argue that the transit noise is likewise important in high stability CPT clocks.

4. Transit noise in microcells

It is interesting to extend the evaluation of the transit noise also to microcell devices. We then consider a typical microcell device as that described in Boudot *et al*'s work [29]. Specifically, we consider a cell containing Cs atoms and Ne as buffer gas at a pressure of 75 Torr (diffusion coefficient $D = 2 \times 10^{-4}\,{\rm m}^2\,{\rm s}^{-1}$). According to [30], the broadening rate for Cs D_1 line with Ne buffer gas can be estimated about 10.85 MHz/Torr, therefore for the considered cell the pressure broadening is of the order of 813 MHz. Taking into account also the Doppler broadening (388 MHz), we assume for the resulting excited

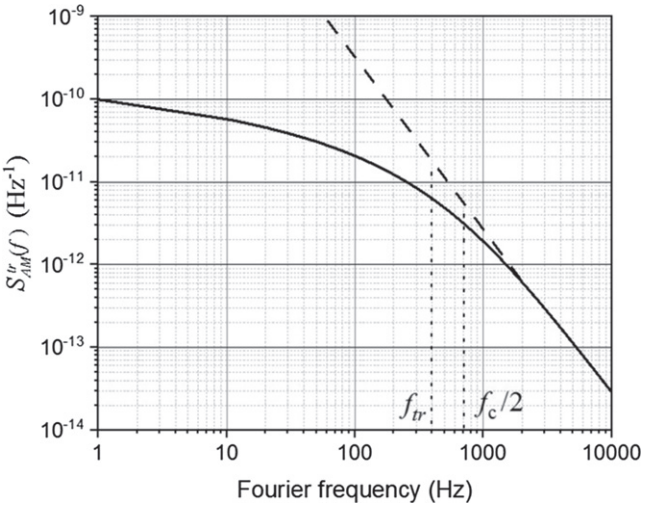

Figure 4. Transit noise spectrum for the microcell considered in the text. The dash line shows the $\sim 1/f^2$ behavior, whereas the dot lines highlight half the cycle frequency (around 750 Hz) and the characteristic frequency $f_{tr} = 400$ Hz.

state relaxation rate the value of $\Gamma^* \approx 2\pi \times 1$ GHz. The hyperfine coherence lifetime is of the order of 260 μs, corresponding to a transversal relaxation rate $\gamma_2 \approx 3800\,\mathrm{s}^{-1}$.

The cell has a diameter of 2 mm and a length of 1.4 mm and works at a temperature of 75 Celsius degrees, corresponding to a density $n = 2.84 \times 10^{18}\,\mathrm{m}^{-3}$. From these values, the optical thickness of the medium turns out $\zeta \approx 3.5$ and $\zeta\gamma_2 \approx 13\,300\,\mathrm{s}^{-1}$. The laser is collimated in a beam with a waist of 0.565 mm and its power at the cell input is 114 μW, corresponding to a pumping rate of $9.3 \times 10^5\,\mathrm{s}^{-1}$, so that the detection takes place in the high laser intensity regime where $\Gamma_p(0) \gg \zeta\gamma_2$.

With the timing sequence adopted in the experiment ($\tau_d = 10\,\mu$s and $T_c = 670\,\mu$s), a contrast of 4% and a linewidth of about 1.6 kHz for the central Ramsey fringe have been measured.

To evaluate the transit noise spectrum, we observe that $f_{tr} = \frac{2D}{\pi w^2} = 400$ Hz for the considered microcell and $f_c/2 \approx 750$ Hz, being $f_c = 1/T_c$ the cycle frequency. Therefore, the pure random-walk approximation does not apply in this case and we have to resort to the complete form of the spectrum expressed by (4) and shown in figure 4. The contribution of the transit noise to the clock Allan deviation is calculated through (16) which yields:

$$\sigma_y^{\mathrm{tr}}(\tau) \approx 6.8 \times 10^{-12}\tau^{-1/2}. \tag{24}$$

The shot noise for the considered cell is calculated with (14) and (18), knowing that the power reaching the detector is of the order of 50 μW [31]; it turns out:

$$\sigma_y^{\mathrm{shot}}(\tau) \approx 2.5 \times 10^{-12}\tau^{-1/2}. \tag{25}$$

We observe that in this specific example the transit noise turns out to be even larger than the shot noise and could become significant for the clock frequency stability when laser frequency and amplitude noises will be reduced [32–34].

5. Conclusions

In conclusion, in this paper we have studied how the frequency stability of vapor cell frequency standards is affected by the Brownian motion of the atoms. The atomic diffusion through the buffer gas induces amplitude fluctuations in the detected signal. The spectrum of this so called transit noise has been already calculated and experimentally verified in [13]. In this work we extended Aoki *et al*'s results to vapor cell clocks, including the role played by the atomic density and taking into account that most performing cell clocks work in pulsed regime.

The transit noise contribution has been calculated for two specific clock arrangements: a high-performing Rb POP clock with a centimeter scale cell and a Cs microcell clock adopting a PCPT scheme. In the first case, the transit noise is in the low 10^{-14} region and is comparable with other sources of amplitude fluctuations, like shot and RIN noises. Also, a possible technological improvement of the laser diodes properties can lead to an improvement of their RIN, making more significant the transit noise contribution.

Similar considerations can be applied to high performing CPT clocks. In fact, we point out that contrasts, atomic quality factors as well as timing sequences, are comparable to those observed in the POP approach. Therefore, we expect that the role played by the transit noise in CPT clocks stability budget is likewise important.

The transit noise magnitude depends on some experimental parameters (mainly beam waist, buffer gas pressure, atomic density), that one may think to tweak to mitigate the effect. Such a strategy, on the other hand, may clash with other noise contributes.

Increasing the beam size is often constrained by power limitations and uniformity issues. A laser beam with a flat-top intensity profile would make the transit noise negligible. However, we point out that during the propagation, the shape of the intensity profile of such a laser usually changes. Taking into account that the physics package of a cell clock includes several layers (thermal and magnetic shields, etc), the beam size and shape hardly remain constant within the length of interest for a clock application. Yet, an increase of the buffer gas pressure certainly results in a reduction of the transit noise but at the same time worsens the cell thermal sensitivity, affecting the stability performances in the medium-long term. Similarly, a reduction of the atom density decreases the resonance contrast and then degrades the short-term stability.

In the example related to a Cs microcell, the transit noise results larger than the shot noise, becoming the actual fundamental limit. However, regardless of the cell size, the main result of our study is that a so far disregarded phenomenon, like the Brownian motion, is actually a source of frequency fluctuations and in some cases might represent the ultimate clock stability limit.

Arguably, the transit noise is expected as well to play a role in continuously operated cell clocks or in devices using coated cells. For these setups, however, a dedicated investigation is required.

We finally note that the effect of the atomic Brownian motion on the clock's stability performances can be interpreted as a mesoscopic physics manifestation in vapor-phase atomic devices. Observed phenomena are not solely associated with the dynamics of individual atoms, but at the same time deals with a scale of physics that is significantly less than the entire vapor volume [35].

References

[1] Godone A, Levi F, Calosso C and Micalizio S 2015 *Riv. Nuovo Cimento* **38** 133
[2] Bandi T, Affolderbach C, Stefanucci C, Merli F, Skrivervik A K and Mileti G 2014 *IEEE Trans. Ultrason. Ferroelectr. Freq. Control* **61** 1769–78
[3] Yun P, Tricot F, Calosso C E, Micalizio S, François B, Boudot R, Guérandel S and de Clercq E 2017 *Phys. Rev. Appl.* **7** 014018
[4] Hafiz M A, Coget G, Petersen M, Rocher C, Guérandel S, Zanon-Willette T, de Clercq E and Boudot R 2018 *Phys. Rev. Appl.* **9** 064002
[5] Liu X, Mérolla J M, Guérandel S, Gorecki C, de Clercq E and Boudot R 2013 *Phys. Rev.* A **87** 013416
[6] Esnault F X, Holleville D, Rossetto N, Guerandel S and Dimarcq N 2010 *Phys. Rev.* A **82** 033436
[7] Langlois M, De Sarlo L, Holleville D, Dimarcq N, Schaff J F and Bernon S 2018 *Phys. Rev. Appl.* **10** 064007
[8] Abdel Hafiz M, Coget G, Yun P, Guérandel S, de Clercq E and Boudot R 2017 *J. Appl. Phys.* **121** 104903
[9] Kang S, Gharavipour M, Affolderbach C, Gruet F and Mileti G 2015 *J. Appl. Phys.* **117** 104510
[10] Micalizio S, Godone A, Levi F and Calosso C 2009 *Phys. Rev.* A **79** 013403
[11] Dong G, Deng J, Lin J, Zhang S, Lin H and Wang Y 2017 *Chin. Opt. Lett.* **15** 040201
[12] Vanier J and Audoin C 1989 *The Quantum Physics of Atomic Frequency Standards* (Bristol: Adam Hilger)
[13] Aoki K and Mitsui T 2016 *Phys. Rev.* A **94** 012703
[14] Gradshteyn I S and Ryzhik I M 2007 *Table of Integrals, Series, and Products* 7th edn (Amsterdam: Elsevier)
[15] Rotondaro M D and Perram G P 1997 *J. Quant. Spectrosc. Radiat. Transfer* **57** 497–507
[16] Godone A, Micalizio S and Levi F 2008 *Metrologia* **45** 313–24
[17] Rubiola E 2008 *Phase Noise and Frequency Stability in Oscillators* (Cambridge: Cambridge University Press)
[18] Godone A, Levi F, Micalizio S and Vanier J 2002 *Eur. Phys. J.* D **18** 5–13
[19] Micalizio S, Calosso C E, Godone A and Levi F 2012 *Metrologia* **49** 425
[20] Steck D 2001 Rb 87 D line data
[21] Ye J, Swartz S, Jungner P and Hall J L 1996 *Opt. Lett.* **21** 1280–2
[22] Vanier J and Mandache C 2007 *Appl. Phys.* B **87** 565–93
[23] Danet J M, Kozlova O, Yun P, Guérande S and de Clercq E 2014 *EPJ Web Conf.* **77** 00017
[24] Calosso C E, Gozzelino M, Godone A, Lin H, Levi F and Micalizio S 2020 *IEEE Trans. Ultrason. Ferroelectr. Freq. Control* **67** 1074–9
[25] Camparo J C 1998 *J. Opt. Soc. Am.* B **15** 1177–86
[26] Kuchina E, Mikhailov E E and Novikova I 2016 *J. Opt. Soc. Am.* B **33** 610–4
[27] Xiao Y, Novikova I, Phillips D F and Walsworth R L 2006 *Phys. Rev. Lett.* **96** 043601
[28] Liu X, Mérolla J M, Guérandel S, de Clercq E and Boudot R 2013 *Opt. Express* **21** 12451–9
[29] Boudot R, Maurice V, Gorecki C and de Clercq E 2018 *J. Opt. Soc. Am.* B **35** 1004–10
[30] Pitz G A, Wertepny D E and Perram G P 2009 *Phys. Rev.* A **80** 062718
[31] Boudot R 2020 private communication
[32] Gerginov V, Knappe S, Shah V, Schwindt P D D, Hollberg L and Kitching J 2006 *J. Opt. Soc. Am.* B **23** 593–7
[33] Kitching J 2018 *Appl. Phys. Rev.* **5** 031302
[34] Knappe S, Shah V, Schwindt P D D, Hollberg L, Kitching J, Liew L A and Moreland J 2004 *Appl. Phys. Lett.* **85** 1460–2
[35] Hudson A and Camparo J 2018 *Phys. Rev.* A **98** 042510